J. Astrophys. Astr. (1989) **10**, 237–255

The 1985 Outburst of RS Ophiuchi: Spectroscopic Results

G. C. Anupama & T. P. Prabhu *Indian Institute of Astrophysics, Bangalore 560034*

Received 1988 October 17; revised 1989 April 13; accepted 1989 April 14

Abstract. Optical spectroscopic data on the recurrent nova RS Ophiuchi obtained between 32 and 108 days after its last outburst on 1985 January 27 are presented. RS Oph was in the coronal-line phase at that time. The widths of the permitted as well as coronal-lines decreased continuously. Assuming that the ejected envelope decelerated due to its interaction with circum stellar matter, its size is deduced as a function of time. Observed fluxes in permitted lines would then imply that the electron density decreased from 3×10^9 cm^{-3} on day 32 to 1.8×10^8 cm^{-3} on day 108, for an assumed filling factor of 0.01. The helium abundance in the ejecta is estimated to be n(He)/n(H) ~ 0.16. The mass of the unshocked ejecta was $3 \times 10\text{-}6$ (ϕ/0.01) $^{1/2}$ $M_\odot$, (at this stage, where f is the filling factor. Observed fluxes in coronal-lines imply that the temperature of coronal-line region decreased from 1.5×10^6 K on day 32 to 1.1×10^6 K on day 108. Most of the coronal line emission, as well as He II emission arises in shocked and cooling ejecta. This region is not isothermal, but contains material at a wide range of temperatures. Mass of the shocked ejecta is estimated to be in the range 10^{-7}–10^{-6} $M\odot$ Based on the number of H- and He-ionizing photons, we estimate that the ionizing source evolved from a radius and temperature of ($2 \times$ l0^{12} cm, 3×10^4 K) on day 32 to ($6 \times$ l0^9 cm, 3.6×10^5 K) on day 204.

We also present the spectra of RS Oph recorded in quiescent phase, 2 and 3 years after outburst, for comparison. The spectrum is dominated by that of M2 giant secondary, with superposed emission lines of H and He I.

Keywords: recurrent novae—optical spectroscopy—nova shells—coronal lines—RS Ophiuchi 1985

1. Introduction

The recurrent nova RS Ophiuchi had its fifth recorded outburst on 1985 January 27. Though it was observed in detail spectroscopically during its previous three outbursts, the 1985 outburst has brought in a wealth of information through observations in the radio, infrared, optical, ultraviolet and X-ray domains. A summary of observations of past outbursts and preliminary results of observations of the 1985 outburst appear in a book form, edited by Bode (1987). We summarize the results below.

RS Oph is an interacting binary system consisting of an M giant and a compact component, with an orbital period of 230 days (Garcia 1986). The interstellar reddening and distance estimates of the system were rather uncertain until ultraviolet

and radio observations were made during the 1985 outburst. The 21-cm H I absorption measurements yield a distance estimate of 1.6 kpc (Hjellming *et al.* 1986). The flux ratio of He II 1640 Å and 3203 Å yields an interstellar reddening of $E(B-V) = 0.73$ (Snijders 1987), a value consistent with H I absorption measure. We will adopt the above estimates of distance and reddening in this paper.

The optical spectrum of RS Oph during outbursts is characterized by strong emission in coronal lines. There is a remarkable similarity between optical spectra of different outbursts. The coronal lines are explained to result from gas which is shock-heated as the ejected envelope expands supersonically into the circumstellar matter accumulated through steady stellar wind (Gorbatskii 1972, 1973). The shock-heated region also emits synchrotron radiation in the radio region (Hjellming *et al.* 1986), and thermal radiation in soft X-rays (Mason *et al.* 1987). The theoretical model of the envelope by Bode & Kahn (1985) is similar in many respects to that of Supernovae, but has much shorter timescales. Coronal as well as other high excitation lines, radio, and X-ray emissions reach a peak at 60 days from the outburst, and then decline. After about 100 days since outburst, a remnant radio and X-ray source is still present. This probably represents the compact component, the radio emission being of gyrosynchrotron origin as in magnetic cataclysmic variables (Hjellming *et al.* (1986). The remnant X-ray radiation implies a temperature of 3.5×10^5 K and luminosity of 10^{37} erg s $^{-1}$ (Mason *et al.* 1987). The inferred blackbody radius of 10^9 cm suggests that the compact remnant is a hot white dwarf, and not a bloated main-sequence star as suggested by Livio, Truran & Webbink (1986).

The VLA as well as VLBI (Hjellming *et al* 1986; Taylor *et al.* 1989) sizes imply an average expansion rate (rate of change of total size) of 0.0026–0.0030 arcsec per day, or expansion velocities of ~ 4000 km s^{-1} at a distance of 1.6 kpc. High initial velocity was also apparent in the optical and ultraviolet lines (Rosino & Iijima 1987; Snijders 1987). The VLBI structure consists of a central component of size 0.06 arcsec, and fainter extension to ±100 milli-arcsec in east-west direction, the thickness ranging from 10–30 milli-arcsec.

Infrared photometric and spectroscopic data have been used by Evans *et al.* (1988) to conclude that there were four components in the remnant: the outer region at 2×10^4 K represents unshocked stellar wind; the two middle regions at $\sim 10^5$ K contain the shocked stellar wind and ejecta; the inner region at 2×10^4 K contains unshocked stellar ejecta. Evans *et al.* also conclude that an additional source of infrared radiation, possibly a hot spot on the accretion disc, was present prior to outburst, vanished soon afterwards, and reappeared subsequently. The middle shocked regions are expected to contain still hotter material that does not contribute to the infrared radiation, but manifests itself through radio, X-ray and coronal emission.

The visual maximum of RS Oph during the 1985 outburst appears to lie between the discovery of outburst on 1985 January 26 and next observation on January 28. We have assumed 1985 January 27.5 as the day of maximum, following Rosino & Iijima (1987).

We present in the next section the spectroscopic data obtained by us between 32 and 108 days from maximum, using the 102-cm reflector of Vainu Bappu Observatory, Kavalur. Based on the permitted lines of hydrogen and helium, we derive in Section 3 the electron densities, the helium abundance, and the mass of the envelope. The coronal-line fluxes are used in Section 4 to derive the temperature of coronal-line-emitting plasma.

2. Spectroscopic data

2.1 *Observations*

Post-maximum spectra in the range 4300–8900 Å were recorded between 1985 February 27 and May 15, using the 102-cm reflector and the Cassegrain spectrograph equipped with a Varo 8605 single-stage image intensifier, at the Vainu Bappu Observatory(VBO), Kavalur. The dispersions of the spectra are 194and 132Å mm^{-1}. The spectra were recorded on Kodak IIa-D plates held in contact with the output fiber-optic faceplate of the image intensifier. All the spectra were calibrated using an auxiliary calibration spectrograph. The stars 57 Ser, 1 Vir and γ Gem were used as Standard stars for the determination of instrumental response corrections. Table 1 gives the details of observations made during the outburst.

Spectroscopic monitoring was continued during quiescence. A few spectra are presented for comparison. The spectra recorded on 1987 March 4 (100 Å mm^{-1}; Kodak IIa-D), and 1988 April 14 and 16 (200 Å mm^{-1}; Kodak 103a-D) were obtained using the Carl-Zeiss UAG spectrograph, equipped with the Varo 8605 image intensifier.

2.2 *Data Reduction*

The spectrograms were digitized at 35 μm intervals using 7.5–10 μm wide apertures on the Perkin-Elmer PDS 1010 M microdensitometer at the Indian Institute of Astrophysics (IIA), Bangalore, and analysed using the software RESPECT (Prabhu, Anupama & Giridhar 1987) at the VAX 11/780 installation at VBO.

Photographic grain noise was filtered using a low-pass filter (cutoff = 15 cycles mm^{-1}) in Fourier space. The intensity calibration was determined as a third-degree polynomial in Baker density and log (relative intensities). The wavelength scale was determined using a Fe + Ne comparison source spectrum. The stellar spectrum was brought to a linear wavelength scale by cubic spline interpolation. The

Table 1. Journal of observations.

UT 1985		Wavelength range Å	Dispersion Å mm^{-1}
Feb	27.99	6300–8900	194
Mar	27.89	6300–8900	194
	27.93	6300–8900	194
	27.97	6300–8900	194
	28.89	4300–5600	132
	28.95	4300–5600	132
	28.99	5000–7600	132
Apr	26.96	6300–8900	194
	28.86	5700–8000	194
	28.99	6300–8900	194
May	15.87	6300–8900	194
	15.94	5700–8000	194

instrumental response curve was obtained using the standard star spectrum and applied to the nova spectrum. The atmospheric absorption bands in the near-infrared were removed by the following method: The continuum ranges in the standard star devoid of the telluric bands were set to zero on a log (intensity) scale, the stellar lines were also set to zero, and the spectrum brought to unit airmass. This template spectrum was then multiplied by a suitable constant such that after subtraction in log (intensity) the atmospheric features in the nova spectrum were smoothed out. The spectra were then flux calibrated using the SAAO *BVRI* photometric observations (P. Whitelock 1988, personal communication; D. Kilkenny 1988, personal communication). Instrumental *BVRI* magnitudes were obtained using standard *B* (Allen 1973) and *VRI* response curves (Bessell 1986). A correction curve was computed from the photometric data and applied to the observed spectrum to bring it to a log (flux) scale.

Data at the edges of the plates are generally noisy and affected by image-tube distortion, rendering correction in these areas uncertain. The derived fluxes of the emission lines have an overall error of 20 percent, with larger errors at the edges and for weaker lines. The Hα emission line is overexposed on some of the plates, particularly so on 1985 April 28.99, where adjacency effect is noticeable. An average value of the fluxes is taken for each epoch with less weight being given to the overexposed lines. The wavelength calibration in the region 4300–4800 Å is inaccurate due to the comparison lines not being registered. However, line identifications have been made by comparing our spectrum with the spectrum of Rosino & Iijima (1987). The region around Hγ is noisy and poorly resolved due to image-tube distortion. Instrumental response correction was not satisfactory in a few cases and the fluxes in these instances have not been used in the analysis.

2.3 *Description of Spectra*

Spectroscopic observations of RS Oph were made at VBO at phases (i) 32 days after maximum when the nova had declined to $V \sim 8.8$, (ii) 59 and 60 days after maximum at $V \sim 9.8$, (iii) 89 and 91 days after maximum at $V \sim 10.5$, and (iv) 108 days after maximum at $V \sim 10.9$. The spectra are shown in Figs 1–3. Tables 2 and 3 list the line fluxes at each phase. Line identifications have been made based on the identifications of Dufay *et al.* (1964), Rosino & Iijima (1987), Wallerstein & Garnavich (1986), and using the catalogue of Meinel, Aveni & Stockton (1975). In the following, spectra at each phase are described.

Phase 32 (1985 Feb. 27): The spectrum is characterized by strong, broad emission lines. The prominent lines are Hα, He I 6678, 7065, 7281; O I 7774 and 8446, λ 8446 being very much stronger than λ 7774. He II 7593 is also present. The coronal-lines [Fe X] 6374 and [Fe XI] 7892 are fairly strong, whereas [A XI] 6919 is barely visible. Paschen lines P_{11} 8863 and P_{12} 8750 are strong. P_{13} 8665, P_{15} 8445 and P_{16} 8502 are blended with the Ca II (2) triplet at 8662, 8542 and 8498 Å. P_{14} 8598 is blended with N I(3) 8594. He II 8236 could be present blended with N I (2) 8184–8242 complex. N I (1) 8680–8719 and N I (3) 7423–7442 could also be present. The lines of Fe II (72, 73) are also present with Fe II (73) 7711 being strong. The feature at 6830 Å, identified with [Kr III] 6826.9 by Joy & Swings (1945) is also fairly strong.

Phase 59 and 60 (1985 Mar. 27, 28): The lines have narrowed and the degree of excitation increased, as seen from the strengthening of the coronal-lines and He II lines.

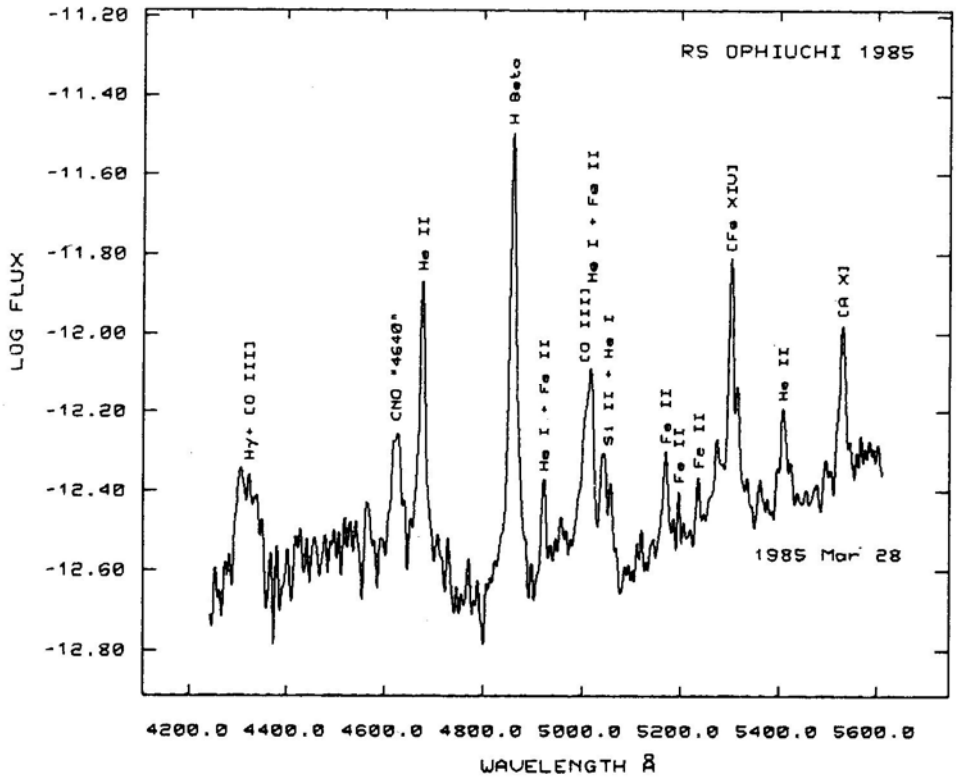

Figure 1. Spectrum of RS Oph on day 60 in the range 4250–5600 Å. Note the strength of coronal and He II lines. Flux is in units of erg cm^{-2} s–1 $Å^{-1}$.

Shortward of 6300 Å, the most prominent lines are H*β* ,He I 5876, He II 4686; the coronal lines [Fe XIV] 5303 and [A X] 5535. Moderately strong are [N II] 5755, the CNO "4640" complex, lines of Fe II (42), He II 5411, [O III] 4363, 4959, 5007; *Hγ,* Si II 5041, 5056. He I 4922, 5016 are blended with Fe II (42) lines at 4924 Å and 5018 Å respectively; and He I 5047 is blended with Si II lines. Also present are the lines of Fe II (48, 49), [Ni XIII] 5116, [Fe VII] 6086, and [K IV] 6101.

Phase 89 and 91 (1985 Apr. 26,28): The lines have generally decreased in strength and excitation has decreased. The lines of Hα, He I 5876, 6678, 7065, [N II] 5755 are the most prominent lines. O I 8446 is also strong although O I 7774 has faded to near invisibility. Among the coronal lines, [Fe X] 6374 and [Fe XI] 7892 are prominent, whereas [A XI] 6919 has weakened considerably. He II, Fe II, and N I lines have also considerably weakened. Moderately strong are the lines of [O I] 6300, [Fe VII]6086, [K IV] 6101 and the feature at 6830 Å. [O II]7319–7333 is just visible. The TiO absorption band at 6158 Å arising in the M-giant secondary spectrum begins to appear.

Phase 108 (1985 May 15): There is an overall decrease in the emission-line strengths. The degree of excitation has further decreased, with most of the high excitation lines fading. The coronal lines of [Fe X] and [Fe XI] are however still present, whereas [A XI] has almost disappeared. The prominent emission lines in the order of decreasing

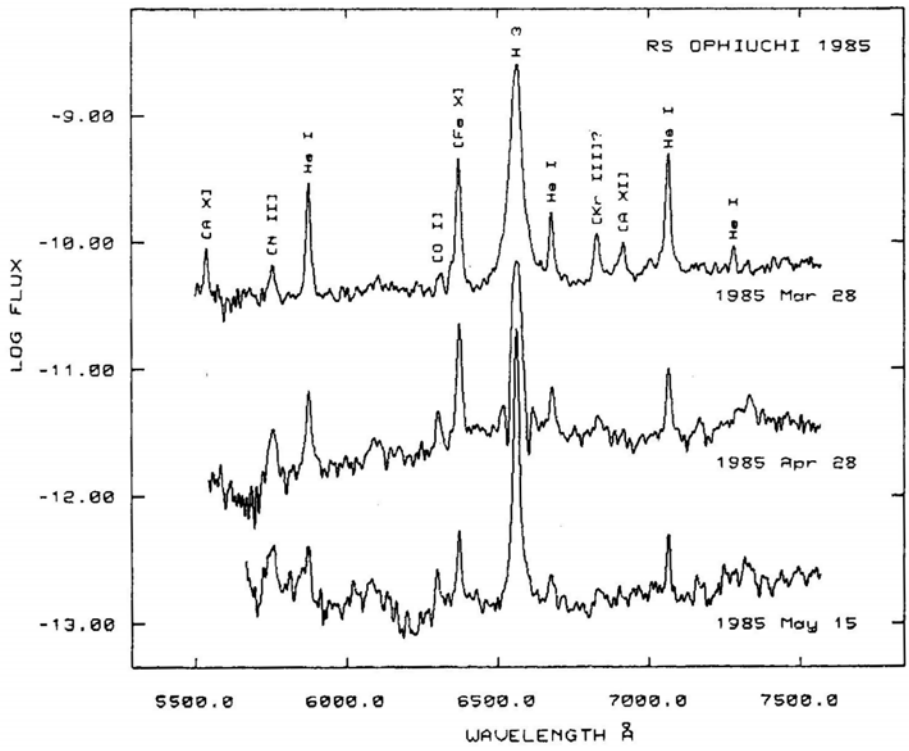

Figure 2. Spectra of RS Oph on days 60, 91, and 108, in the range 5600–7500 Å. Hα was overexposed on April 28. Instrumental response correction on May 15 is uncertain shortward of 6200Å. Note the fading of coronal and He I lines, and brightening of [O I] and [N II] lines. Flux is in units of erg cm^{-2} s^{-1} $Å^{-1}$. Top two spectra are shifted upwards by three and one unit respectively in log (flux).

strengths are Hα, [N II] 5755, He I 5876, O I 8446, [O I] 6300, [O II] 7319–7333, He I 7065, [Fe XI] 7892, He I 6678 and [Fe X] 6374. Underlying the emission-line spectrum is that of the M-giant secondary.

Fig. 4 shows spectra obtained during quiescence on 1987 March 4 and 1988 April 16. The spectrum during minimum is dominated by that of the M-giant secondary, with superposed emission lines. The 1987 spectrum shows clearly the emission lines of H*β*, He I 5876 and Hα. In the 1988 spectrum, Hα is prominently visible; H*β* and He I 5876 are weak. Lines of Fe II could be present in both spectra, but underexposure of the spectrograms makes identifications difficult. Table 4 lists the fluxes of *Hβ,* Hα and He I 5876 in 1987 March and 1988 April. The values for 1988 April are averages of the ones measured on April 14 and 16.

3. Physical conditions in the envelope

Bode & Kahn (1985) have modelled the evolution of the envelope of RS Oph using the early radio and X-ray observations. They estimate that free expansion phase lasted

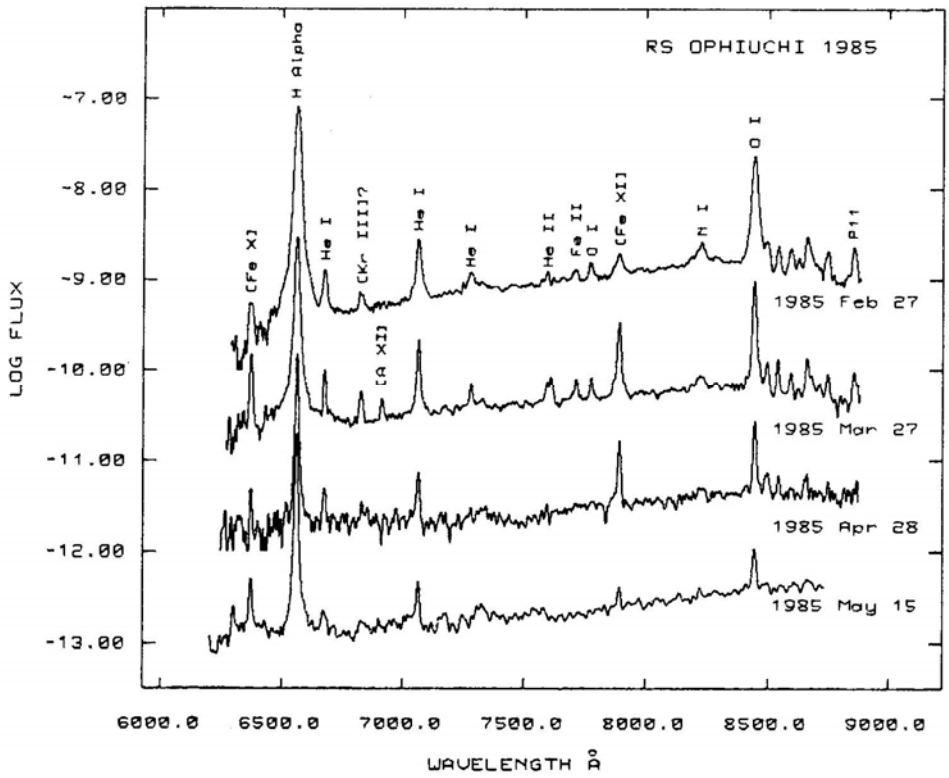

Figure 3. Spectra of RS Oph on days 59,91, and 108, in the range 6250–8900 Å. He II 7594 is probably overestimated by overcorrection for atmospheric absorption. Note the narrowing down of lines with time; increase in the strength of coronal and He I lines till day 59 and their fall thereafter; steady decrease in the strength of H lines and O I 8446. Flux is in units of erg cm^{-2} $s^{-1}Å^{-1}$. Top three spectra are shifted upwards by three, two, and one unit respectively in log (flux).

only a few days, after which the envelope began to expand adiabatically while accreting shock-heated circumstellar matter. Cooling became important after about 60 days. During the latter two phases, the radius and velocity of the envelope vary as

$$r_s = a\,t^{2/3}\,; \qquad v_s = \frac{2}{3} a\,t^{-1/3} \tag{1}$$

and

$$r_s = b\,t^{1/2}\,; \qquad v_s = \frac{1}{2} b\,t^{-1/2} \tag{2}$$

with $a = 3.3 \times 10^{13}$ cm $day^{-2/3}$ and $b = 8.2 \times 10^{13}$ cm $day^{-1/2}$ as estimated by Bode &Kahn.

O'Brien & Kahn (1987) suggest that the wind from the companion reached only 7×10^{14} cm since the last outburst of RS Oph and the envelope ejected during the present outburst would overtake it by day 65. The envelope may thus have never reached the momentum-conserving snow-plough stage. We compare in Table 5 the

Table 2. Line identifications and observed fluxes, in the region 4300–5600 Å, dereddened for E(B – V) = 0.73.

λ_m		Flux (10^{-10} erg cm^{-2} s^{-1})				
Å	Identification	Day	32	59–60	89–91	108
4319*	4340.47 Hγ			1.68		
	4363.21 [O III] (2)					
4565*	4582.84 Fe II (37)					
	4583.83 Fe II (38)					
	4595.68 Fe II (38)			0.32		
4623*	"4640" CNO complex			0.89		
4676*	4685.68 He II (1)			1.84		
4728	4731.44 Fe II (43)			0.18		
4859	4861.33 Hβ			3.67		
4922	4921.93 He I (48)			0.32		
	4923.92 Fe II (42)					
4957	4958.91 [O III] (1)			0.09		
5012	5006.84 [O III] (1)					
	5015.68 He I (4)			1.12		
	5018.43 Fe II (42)					
5044	5041.06 Si II (5)			0.37		
	5047.70 He I (47)					
	5056.00 Si II (5)					
5116	5116.3 [Ni XIII] (1)			0.08		
5168	5169.03 Fe II (42)			0.20		
5196	5197.57 Fe II (49)			0.09		
5236	5234.62 Fe II (49)			0.10		
5274	5275.99 Fe II (49)			0.10		
	5276.10 [Fe VII] (2)					
5302	5302.86 [Fe XIV] (1)			1.04		
5315	5316.61 Fe II (49)			0.22:		
	5316.78 Fe II (48)					
5362	5362.86 Fe II (48)			0.09		
5409	5411.52 He II (2)			0.32		
5495	5495.82 [Fe II] (17)			0.11		
5530	5534.60 [A X] (1)			0.78		

Multiplet numbers appear in parantheses.
* Wavelength calibration is inaccurate due to comparison lines not being registered in this region. Lines have been identified based on a comparison of our spectrum with that of Rosino & Iijima (1987).

velocities derived from Equation (1) and those observed as fullwidths at half maximum of permitted as well as coronal lines. There were no significant differences between the widths of permitted and coronal lines. The lines affected by blending have been left out. The tabulated values have been corrected for an average velocity resolution of 300 km s^{-1}, corresponding to the spectra used. The observed values are slightly smaller than predicted between days 60–108. This suggests that the constant a is a slight overestimate, the formal value based on our velocities being (2.7 ± 0.5) $\times 10^{13}$ cm day $^{-2/3}$.

Table 3. Line identifications and observed fluxes, in the region 5700–8900 Å, dereddened for $E(B–V) = 0.73$.

λ_m		Flux (10^{-10} erg cm^{-2} s^{-1})			
Å	Identification	Day 32	59–60	89–91	108
5755	5754.80 [N II] (3)		0.24	0.32	0.30
5874	5875.63 He I (11)		1.05	0.57	0.17
6084	6085.50 [Fe VII] (1)		0.03	0.18	0.06
6104	6101.10 [K IV] (1)		0.05	0.20	0.05
6301	6300.23 [O I] (1)		0.03	0.19	0.16
6346	6347.10 Si II (2)		0.08	0.06	0.04
6372	6374.51 [Fe XI]	0.54	1.30	1.75:	0.28
	6363.00 [O I] (1)				
6562	6562.82 Hα	107.43	29.22	9.26	3.78
6676	6678.15 He I (46)	0.81	0.43	0.21	0.13
6828	6826.90 [Kr III] (1)	0.30	0.26	0.12	0.05
6917	6919.10 [A XI] (1)	0.05	0.14	0.07	0.06
7063	7065.19 He I (10)	1.98	1.27	0.60	0.21
7279	7281.35 He I	0.42	0.17	0.06	0.03
7328	7310.24 Fe II (73)				
	7320.70 Fe II (73)	0.12	0.07		
	7318.60 [O II] (2)				
	7319.40 [O II] (2)				
	7329.90 [O II] (2)				
	7330.70 [O II] (2)			0.13	0.15
7455	7423.63, 7442.28,				
	7468.29 N I (3)				
	7462.38 Fe II (73)				
	7515.88 Fe II (73)	0.11	0.13	0.07	
7593	7592.74 He II (6)	0.18	0.35	0.06	0.03
7711	7711.71 Fe II (73)	0.26	0.14	0.02	
7773	7771.96, 7774.18				
	7775.40 O I (1)	0.46	0.19	0.06	0.02
7890	7891.94 [Fe XI] (1)	0.71	1.56	0.67	0.18
8187	8184.80, 8187.95,				
+	8216.28, 8223.07,				
8226	8242.34 N I (2)				
	8236.77 He II (6)	0.86	0.29	0.14	0.05
8444	8446.35 O I (4)				
	8446.76 O I (4)	16.38	4.20	0.83	0.37
8500	8498.02 Ca II (2)				
	8502.49 H P_{16}	0.76	0.37	0.09	0.06
8543	8542.09 Ca II (2)				
	8545.38 H P_{15}	0.60	0.33	0.07	0.03
8596	8594.01 Ca II (2)				
	8598.39 H P_{14}	0.58	0.20	0.08	0.03
8627	8629.24 N I (8)	0.16	0.07	0.05	0.03
8665	8662.14 Ca II (2)				
	8665.02 H P_{13}	0.85	0.43	0.10	0.04
8680	8680.24, 8683.38,				
	8686.13 N I (1)	0.20	0.14	0.03	0.02
8715	8703.24, 8711.69,				
	8718.82 N I (1)	0.11	0.10	0.05	0.02
8745	8750.48 H P_{12}	0.49	0.18	0.08	0.03:
8859	8862.77 H P_{13}	0.49	0.22	0.09	0.05:

Multiplet numbers appear in parantheses.

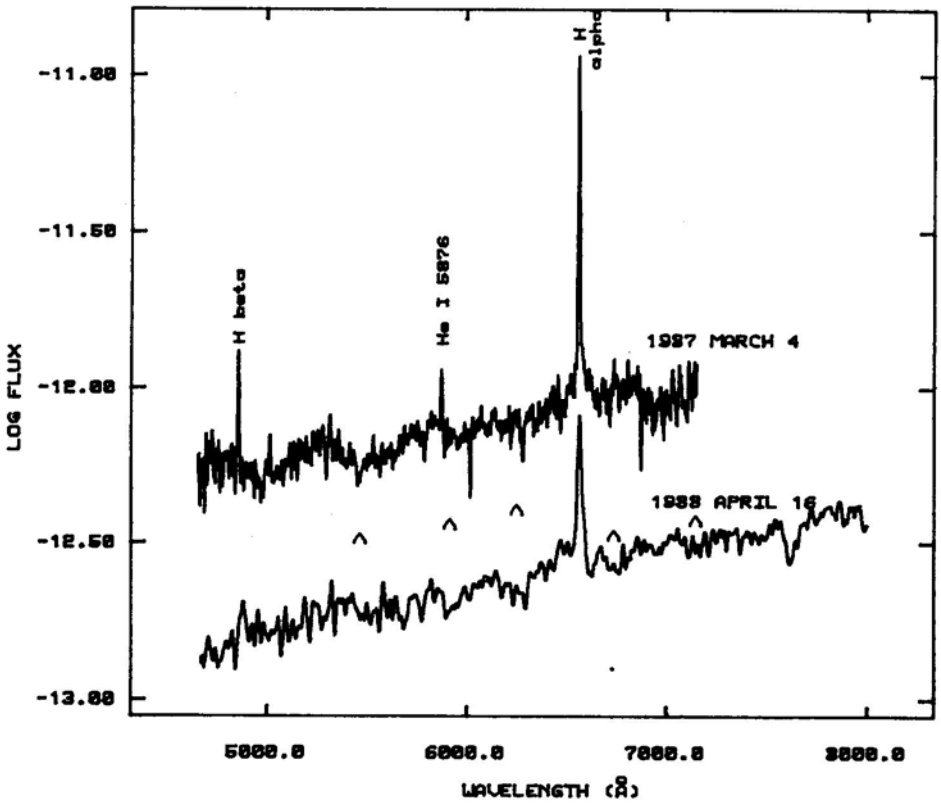

Figure 4. Quiescent spectrum of RS Oph on 1987 March 4 (100 Å mm^{-1}) and 1988 April 16 (200 Å mm^{-1}). Flux is in units of erg cm^{-2} $s^{-1}Å^{-1}$. Top spectrum is shifted upwards by one unit in log (flux). The TiO absorption bands in the secondary spectrum are marked as A.

Table 4. Emission line fluxes in the spectra of RS Ophiuchi during minimum.

λ_m		Flux (10^{-10} erg cm^{-2} s^{-1})	
Å	Identification	1987 Mar 4	1988 Apr 14–16
4862	4861.33 Hβ	0.25	0.18
5874	5875.64 He I	0.08	0.05:
6561	6562.82 Hα	1.53	0.77

3.1 *Electron Density and Envelope Mass*

Forbidden emission lines are rather weak in our spectra and are generally blended with other lines. [O I] 6300 and [N II] 5755 are the only clearly resolved lines. We have hence not attempted to use the forbidden lines to estimate the electron density and temperature. Instead, we assume a temperature $T_e = 1.5 \times 10_4$ K consistent with the

Table 5. The expansion velocity, electron density and mass of the envelope

Day	V_e(km s^{-1}) Obs.	Model	n_e 10^8 cm^{-3}	M_H 10^{-6} $M_\odot$
32.0	836±192	792	30.6	3.7
59.9	470±107	643	8.8	3.5
90.7	424±127	560	3.4	3.0
108.4	431±99	527	1.8	2.3

estimates of Evans *et al.* (1988), and derive the electron density from Hα line using the relationship,

$$n_e n_{H^+} = \frac{4\pi D^2 f_\alpha}{a(3,2)\, h\nu V}. \tag{3}$$

We assume $n_e = n_{H^+}(1 + N_{He^+}/N_{H^+} 2N_{He^{++}}/N_{H^+})$ with the ion abundances of He^+ and He^{++} derived in the next section. In Equation (3), D is the distance to RS Oph, f_α is the observed Hα flux, $h\nu$, the Hα photon energy, $a(3,2) = f(n_e, T_e)$ is the effective recombination coefficient for the transition, and V is the line-emitting volume. We proceed to estimate the hydrogen mass of the envelope

$$M_{H^+} = n_{H^+} m_H V \tag{4}$$

where m_H is the mass of H atom. The volume is estimated as

$$V = \frac{4}{3}\pi r_s^3 \phi \tag{5}$$

where ϕ is the filling factor.

VLBI observations of RS Oph (Taylor *et al.* 1989) indicate that the envelope was disc-shaped rather than spherical. Most of the radio emission originated from a compact component with an angular size of 60 mas on day 77. Equation (1) predicts a comparable value of 49 mas. Though an expanding ring or disc may not follow Equation (1), the above agreement, together with the agreement with expansion velocities, encourages us to follow the model. We will use a value of filling factor $\phi = 0.01$ corresponding to a ring of width a tenth of its radius, and covering a tenth of the surface of the sphere of the same radius. The volume of the envelope is then derived by

$$V = 1.45 \times 10^{39}\, t_d^2 \text{ cm}^3 \tag{6}$$

where t_d is time measured in days since outburst.

We computed electron densities in the envelope using the above expressions for volume, the Hα fluxes from our data, and recombination coefficients tabulated by Hummer & Storey (1987). The computed electron densities are listed in Table 5. We also computed electron densities using our data on Hβ on day 60, P_{11}, P_{12} on all the days, and the data of Evans *et al.* (1988) on Pα, Brγ and Brδ. Brδ appeared much brighter than expected, possibly due to a blend with [Si VI] 1.961 μm (Evans *et al.* 1988). Brγ was also somewhat brighter than expected till day 60. Our data on P_{11} and

P_{12} fluxes are rather uncertain, particularly so after day 60. Hβ was fainter than expected on day 60.

One may proceed to calculate the optical depth in Lyα assuming the density derived above, the thickness following our model, and for a neutral fraction of hydrogen 10^{-2}. The derived optical depth decreases from 4×10^7 on day 32 to 5×10^6 on day 108. Radiative recombination calculations of H spectrum are not valid at such high optical depths in Lyα. Indeed on day 59.9, we find the ratio of Hα/Hβ to be nearly 8.0 instead of 2.62 predicted by radiative recombination case for appropriate density and temperature (Hummer & Storey 1987). Similarly Pα / Hβ = 0.105 (against 0.0236).

The effect of high optical depths in Lyman and Balmer lines have been incorporated in calculations of H spectrum by several workers in an attempt to compare with the spectra of active galactic nuclei. Our observed line ratios match well with the model BD3 of Krolik & McKee (1978) for an ionization parameter 10^{-2}, electron temperature 1.6×10^4, electron density 10^9 and Lyα optical depth 10^5. Among the models of Drake &Ulrich (1980), the high optical depth and high dilution of incident radiation reproduces our observed ratios. We note here that the dilution factor for radiation in RS Oph beyond the first few days is much smaller than encountered in active galactic nuclei.

The above models predict a lower value of Hβ emissivity compared to the radiative recombination case. However, the emissivity of Hα differs by less than 50 per cent, and hence our derived electron densities would change by less than 25 per cent.

The mass of hydrogen in the envelope, as derived from Equation (4) is also listed in Table 5. The derived value is steadily decreasing. On the other hand, the total mass of the envelope is expected to steadily rise due to accretion from the circumstellar matter. The newly accreted matter is heated to coronal temperatures as it passes through the shock at the edge of the envelope. The hot matter does not contribute significantly to the recombination spectrum. Since the cooling rate is low during the adiabatic phase, one expects the permitted lines to arise mostly from the ejected envelope, and hence the derived mass should have remained constant. The inferred mass varies as the square root of the emitting volume, and hence it would appear that the volume has increased faster than indicated by the assumed model. If the filling factor is made to increase as $t^{\circ}\ {}^{6}{}_{\mathrm{d}}$ instead of being held constant, the inferred mass will remain constant. This may arise either due to a diffusing out of the thickness of the ring at a rate faster than expected from homologous expansion, or if the emitting gas was initially in the form of condensations which diffused out in time.

Our estimates of the mass of the ejecta agree with the estimate of Bohigas *et al.* (1989) which is based on the total mass of the envelope derived at late stages when most of the shocked matter had cooled down.

It is difficult to estimate the volume of the envelope during quiescence in 1987 and 1988. The envelope would have overtaken the stellar wind by day 65 (O'Brien & Kahn 1987), and one does not expect much deceleration thereafter. Assuming that the envelope expanded with a constant velocity of 400 km s $^{-1}$, we estimate that the electron densities were $\sim 10\ ^{7}\mathrm{cm}^{-3}$ in 1987–88 and the mass of the envelope $\sim 10^{-5}\ M_{\odot}$. This electron density is higher than estimated by Bohigas *et al.* (1989) for day 204, but the mass estimate is comparable. Uncertainties in the emitting volume, and possible contributions to the emission flux from the accretion disc affect our estimates.

3.2 *The Helium Abundance*

The helium abundance can be estimated using the lines of He I and He II in relation to H, if we assume that He is either singly or doubly ionized all through the H^+ region. Evans *et al.* (1988) suggest that He II lines originated in the cooling shocked matter at a temperature of ~2 $\times 10^5$ K, during the early months after outburst. Thus the derived He abundance would be reliable only at later epochs.

The collisional effects on the 2^3S level need to be taken into account for He I. We do this applying the interpolation formulae of Clegg (1987), as corrections to the emissivities of Brocklehurst (1971). We have extrapolated Brocklehurst's values logarithmically to the densities of our interest, at an assumed electron temperature of 1.5×10^4 K. Clegg recommends that He I 6678 is the best line for use in abundance determinations. We find that He I 7065 agrees with 6678 Å line. Hence we use both these lines, excluding 6678 Å line on day 108 when its intensity was very uncertain. He I 5876 yields much lower abundance as found also by Bohigas *et al.* (1989). The He^+/H^+ abundances determined by us using He I 6678, 7065 and Hα are listed in Table 6. The value for day 204 is based on He I 6678/Hα data of Bruch (1986).

The coronal lines were very faint by day 201, and we may assume that He II emission originated in unshocked ejecta. Using He II 4686/H*β* from Bohigas *et al.* (1989) and the tables of Hummer & Storey (1987) we obtain a He^{++}/H^+ abundance of 0.05. This together with $He^+/H^+ = 0.11$ yields a helium abundance

$$n(\mathrm{He})/n(\mathrm{H}) = 0.16$$

3.3 *Radius and Temperature of the Ionizing Source*

Theoretical models of thermonuclear runaways on white dwarfs suggest that during the constant bolometric luminosity phase following an outburst, the radius of the ionizing source decreases whereas the effective temperature increases (Starrfield, Sparks & Truran 1985). Similar results have been obtained from observations of envelopes of classical novae (Ferland 1979; Krautter & Williams 1988; Martin 1988). We will estimate in the following, the radius and temperature of the ionizing source in RS Oph, based on an estimate of the number of ionizing photons.

With $Q(X, T_s)$ as the number of photons that can ionize species X at a temperature T_s of the source, we have

$$\frac{Q(\mathrm{He}^0, T_s)}{Q(\mathrm{H}^0, T_s)} = \frac{\alpha_B(\mathrm{He}^0)}{\alpha_B(\mathrm{H}^0)} \cdot \frac{N(\mathrm{He}^+)}{N(\mathrm{H}^+)} = 1.067 \frac{N(\mathrm{He}^+)}{N(\mathrm{H}^+)}, \tag{7}$$

and

$$\frac{Q(\mathrm{He}^+, T_s)}{Q(\mathrm{He}^0, T_s)} = \frac{\alpha_B(\mathrm{He}^+)}{\alpha_B(\mathrm{He}^0)} \cdot \frac{N(\mathrm{He}^{++})}{N(\mathrm{He}^+)} = 5.75 \frac{N(\mathrm{He}^{++})}{N(\mathrm{He}^+)}. \tag{8}$$

In these equations, α_B denotes the Case B recombination coefficient and $N(X)$, the total number of ionized particles X.

We estimate various Q values assuming blackbody spectra. Using $N(He^+)/N(H^+)$ we derive temperatures of 3.2×10^4 K on day 32 and 4.3×10^4 K on day 60. For

temperatures in excess of 4×10^4 K, both He and H compete for ionizing photons and He^+ and H^+ Strömgren spheres coincide (Osterbrock 1974). The estimate for day 60 is hence a lower limit. If we further assume that no He^{++} existed in the permitted-line region, we obtain an upper limit of $\sim 10^5$ K.

Beyond day 60, we assume that a reduction in He^+/H^+ below 0.16 is to be compensated by He^{++}/H^+. Using the implied values of $N(He^{++})/N(H^+)$ we obtain the temperatures of 1.5×10^5 K (day 90.7), 2.6×10^5 K (day 108.4) and 3.6×10^5 K (day 201). The last estimate agrees with that of Mason *et al.* (1987) for day 250 based on X-ray data.

The radius of the source R_s can now be estimated using Hα luminosity as

$$Q(\mathrm{H}^0)\,\delta \equiv 4\pi R_s^2\, q(\mathrm{H}^0)\,\delta = \frac{L(\mathrm{H}\alpha)\,\alpha_\beta(\mathrm{H}^0)}{h\nu a(3,2)} \tag{8}$$

where δ is the fraction of photons intercepted by the envelope. We list in Table 6 the radii derived for two values of δ, *viz.,* 0.1 and 1. For day 201, we have used the Hβ luminosity based on Bohigas *et al.* (1989).

The blackbody luminosity of the ionizing source, estimated from R_s and T_s, is also listed in Table 6. There is a sudden drop in the luminosity between days 60 and 90.

4. The coronal lines

Coronal lines appear in the spectrum of RS Oph during the nebular phase, reaching their maximum intensity between days 50–100 (Joy & Swings 1945; Griffin & Thackeray 1958; Dufay *et al.* 1964; Rosino 1987; Rosino & Iijima 1987; Wallerstein & Garnavich 1986). Coronal lines of [Fe X] 6374, [Fe XI] 7892 and [A XI] 6919 were seen in our red-infrared spectra. Spectra recorded on day 60 in the wavelength range 43000-5600 Å showed strong [Fe XIV] 5303 and [A X] 5535 lines. The lines of [Ni XIII] 5116, [Ni XI] 6033, 6346 and [Ni XV] 6702 observed by Wallerstein & Garnavich (1986) can be identified only with difficulty in our spectra due to poor signal-to-noise ratio.

The emissivity(total emission per unit volume, per unit time) in a coronal-line can be expressed as

$$j_L = n_H A f(X, T_e) f_j(n_e, T_e)\, A_{jk}\, h\nu_{jk}, \tag{9}$$

Table 6. The He abundance and physical parameters of the ionizing source.

Day	N_{He^+}/N_{H^+}	$N_{He^{++}}/N_H^*$	T_s 10^5 K	$R_s(10^{10}$ cm) $\delta=0.1$	$\delta=1$	$L_s(10^{38}$ erg s^{-1}) $\delta=0.1$	$\delta=1$
32.0	0.05	0.00	0.32	200	63	29	3.0
59.9	0.12	0.00	>0.43	<44	<14	28:	2.9:
90.7	0.15	0.01	1.50	4.0	1.3	5.5	0.6
108.4	0.13	0.03	2.6	1.6	0.5	8.5	0.9
204.0$^+$	0.11	0.05	3.6	0.6	0.2	5.0	0.5

* The value for day 204 is derived from observations, the rest of the values are assumed ones.
$^+$ Mean epoch of observations of Bohigas *et al.* (1989) and Bruch (1986).

where n_H is the hydrogen number density, A is the abundance of the element, $f(X, T_e)$ is the fraction of the element in the ionization state of interest, f_j is the fraction of ions in the upper level of coronal transition, A_{jk} the transition probability, $h\nu_{jk}$ the energy of the emitted photon.

If one considers ratios of lines due to the same element in different ionization states, then n_H and A cancel out. $f(X, T_e)$ and $f_i(n_e, T_e)$ can be computed and the consequent theoretical line ratios can be compared with the observed ones. In our theoretical computations, we have used the ionization equilibrium calculations of Jacobs *et al.* (1977) for iron, and of Landini & Fossi (1972) for argon. The level populations were determined by cascade-matrix method, modifying the FIVEL program of de Robertis, Dufour & Hunt (1987). The atomic data were taken from Mason (1975) for iron, and from Bhatia, Feldman & Doscheck (1979) for [A XI]. The transition probability for [A X] 5535 Å was from Kastner (1976), and the collision strength was taken to be 0.127 from Czyzak, Aller & Euwema (1974). This value is nearly twice as large as the value used by Wallerstein & Garnavich (1986), but agrees with a smooth interpolation along the corresponding iso-electronic sequence.

It was shown by Mason (1975) that collisional excitation by protons is important under coronal conditions. We have included proton collision using the data available in the sources listed. Since the proton collision strengths were not available for [A X] 5535 line, we computed the value to be

$$\alpha_p = 10^{-10}(-1.43 + 3.52T_6 - 0.5T_6^2 - 0.024T_6^3); \qquad 0.5 \leqslant T_6 \leqslant 2,$$

where T_6 is the electron temperature in units of 10^6 K, following the method of Kastner (1977), and Kastner & Bhatia (1979), using the radial intergrals listed by Kastner (1977).

Mason (1975) has also shown the importance of stimulated absorption of photospheric radiation under coronal conditions. We have formally introduced stimulated absorption in our computations, though because of the high dilution factor, its effect is negligible in our case.

The level populations are very sensitive to the electron density. If the coronal lines arise mainly in the shocked circumstellar matter, following the model of Bode & Kahn (1985) we expect electron densities of 10^6, 5×10^5, 3×10^5 and 2×10^5 cm^{-3} at the four epochs. In order to produce the observed line intensities at such densities, one requires more than 10^{-4} $M_\odot$ of shocked matter assuming solar abundances of iron. An overabundance of iron by a factor greater than 100 will be needed to bring down the mass of the shocked wind to a value consistent with the estimates of Bode & Kahn. On the other hand, if the lines arise in the shocked ejecta, the densities will be larger, and the. observed emission can be explained by $\lesssim 10^{-6}$ $M_\odot$ of shocked matter. We thus conclude that coronal lines originate mostly from shocked ejecta. We will hence assume that the density of the coronal-line-emitting region is similar to that of unshocked ejecta.

The theoretical line-intensity ratios of [Fe XI] 7892/[Fe X] 6374 are plotted in Fig. 5, as a function of electron densities and temperature. Observed ratios are also plotted. The intensities of [Fe X] 6374 were corrected for the contribution due to [O I] 6363, assuming a ratio of [O I] 6300/6363 = 3. The derived temperatures (Table 7) are close to 10^6 K, with a suggestion of slight cooling with time.

On day 60, we could also use [Fe XIV] 5303, [A x] 5535 and [A XI] 6919. We find that the temperature derived from [Fe XIV]/[Fe XI] is higher than that from [Fe XI]/

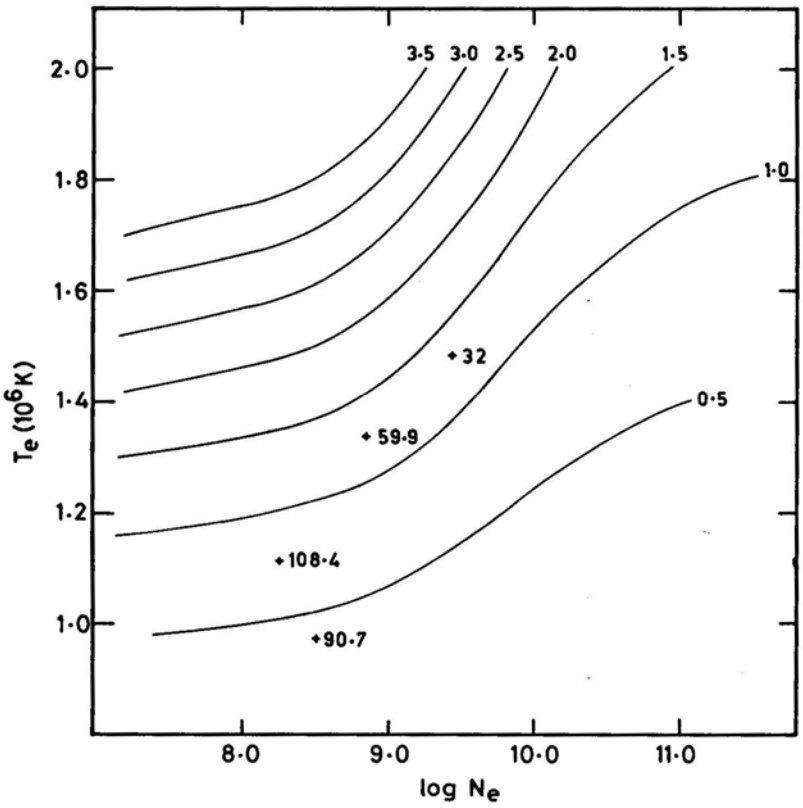

Figure 5. Contours of equal ratios of [Fe XI] 7892/[Fe X] 6374 plotted in (T_e, log Ne) plane. The observed ratios plotted against the assumed densities, indicate the temperature.

Table 7. Electron temperatures of coronal line region.

Day	[Fe XI]/[Fe X]	T_e (10^6 K) [Fe XIV]/[Fe XI]	[A XI]/[A X]
32	1.50		
59.9	1.34	1.52	1.24
90.7	0.98*		
108.4	1.11		

*probably 6374A line strength is overestimated due to uncertain instrumental response correction.

[Fe X], whereas [A XI]/[A X] yields a lower temperature. This indicates that there may be temperature inhomgeneities or gradients in the shocked region. Similar suggestion was also made by Wallerstein & Garnavich (1986).

We have repeated our calculations using the data of Wallerstein & Garnavich (1986) for [Fe X], [Fe XI], [Fe XIV], [A X] and [A XI], after correcting the data for $E(B - V)$

= 0.73. The effect of reduction in reddening, and of using new atomic data, resulted in a reduction of derived temperatures by 512 per cent.

5. Concluding remarks

We have presented optical spectroscopic data on RS Ophiuchi obtained at VBO, Kavalur, between 32 and 108 days since the 1985 outburst of the nova. We have also presented for comparison, spectra of the nova recorded in 1987 March and 1988 April during quiescence. The evolution of the spectrum during this outburst is similar to the past outbursts.

The widths of emission lines agree with the energy-conserving phase of Bode & Kahn (1985) model, though the evolution appears to be slightly faster than predicted by the model. Furthermore, it appears that the shell overtook the circumstellar matter between days 60 and 90 and began to expand with a constant velocity. This agrees with the estimate of O'Brien & Kahn (1987). Thus the momentum-conserving snow-plough stage was probably never reached.

The lines of H and He I arise in the unshocked ejecta. The electron densities (n_e) in the ejecta fell from 3.1×10^9 cm $^{-3}$ on day 32 to 1.8×10^8 cm^{-3} on day 108, for an assumed filling factor of $\phi = 0.01$ (with respect to the entire sphere of radius = radius of the shock). The mass of the ejected envelope was $(3.1 \pm 0.6) \times 10^{-6}\ M_\odot$. For a different filling factor, the density would vary as $\phi^{-1/2}$ and the mass as $\phi^{1/2}$. The smooth fall in the mass of the ejecta derived between days 32 and 108 suggests that ϕ was indeed smaller initially and increased with time, suggesting the presence of diffusive processes.

We derive a helium abundance of n (He)/n(H) = 0.16 following the observations of Bohigas *et al.* (1989) on day 201 and Bruch (1986) on day 207. The small decrease in comparison with the estimate of Bohigas *et al.* is due to the inclusion of collisional effects following Clegg (1987). We will assume, following Evans *et al.* (1988) that significant emission of He II during the early months originated in the shocked, cooling ejecta. Consideration of the number of H-ionizing photons on day 32 confirm that no He^{++} could be present in the photoionized region on that day, and we assume the same to be true also on day 60. He^+ density reaches a maximum on day 90 and falls thereafter. We assume that $[n(He^+) + n(He^{++})]/n(H) = 0.16$ from day 90 onwards. The considerations of H and He ionizing photons thereafter help us in estimating the parameters of the photoionizing source. We estimate that the temperature of the source increased from 3×10^4 K on day 32 to 3.6×10^5 K on day 204. The last estimate agrees with that of Mason *et al.* (1987) based on X-ray observations.

Assuming that the geometrical factors permit only a tenth of the ionizing radiation to be absorbed by the envelope, we derive that the radius of the source decreased from a value of 2×10^{12} cm on day 32 to 6×10^9 cm on day 204. The last radius compares well with the radii of white dwarfs. The implied blackbody luminosity decreased from a value of 3×10^{39} ergs^{-1} on day 32 to nearly a constant value of 6×10^{38} ergs^{-1} between days 90-204.

Most of the coronal-line flux originates in the shocked ejecta. The shocked and cooling ejecta may be comparable in mass to the unshocked ejecta, but a major fraction of these are at temperature of $\sim 10^5$ K which contribute to infrared continuum and He II lines (Evans *et al.* 1988). The observed flux of He II 4686 on day 60 implies a mass of 3×10–$6\ M_\odot$ at $T_e = 10_5$ K and $n_e = 9 \times 108$ cm^{-3}. About $10^{-7}\ M_\odot$ of matter

appears to be at temperatures ~ 1–2 × 10^6 K in which the coronal lines form. The shocked matter has cooled from 1.5 × 10^6 K on day 32 to 1.1 ×10^6 K on day 108, as inferred from [Fe XI]/[Fe X] line ratios. The temperatures deduced from different lines mutually differ by ~ 10 per cent. This is more likely due to temperature gradients in the cooling, shocked ejecta rather than due to uncertainties in our estimates.

Acknowledgements

We are grateful to D. Kilkenny & P. Whitelock for obtaining photometric data of RS Ophiuchi on 1988 April 15 and 19 on our special request. We thank A. Evans and P. Whitelock for providing their data in advance of publication. G. J. Ferland, the referee, enlightened us on the collisional effects in He I spectrum. We are also grateful to A. Evans and M. F. Bode for critically reading an earlier version, as a result of which the paper has immensely benefited. We also acknowledge useful discussions we had with P. K. Raju, D. C. V. Mallik and N. K. Rao.

References

Allen, C. W.1973, *Astrophysical Quantities,* Univ. London.
Bhatia, A. K., Feldman, U., Doscheek, G. A.1979, *Astr. Astrophys.,***80**, 22.
Bessell, M, S. 1986, *Publ. astr. Soc. Pacific,* **98**, 1303.
Bode, M.F.(Ed.) 1987, *RS Ophiuchi*(1985)*and the Recurrent Nova Phenomenon,* VNU Science Press, Utrecht.
Bode, M. F., Kahn, F. D.1985, *Mon. Not. R. astr. Soc.,* **217**, 205.
Bohigas, J., Echevarria, J., Diego, F., Sarmiento, J. A.1989, *Mon. Not. R. astr. Soc.,* **238**,1395.
Brocklehurst, M.1971, *Mon. Not. R. astr. Soc.,* **153**, 271.
Bruch, A. 1986, *Astr. Astrophys.,* **167,** 91.
Clegg, R. E. S. 1987, *Mon. Not. R. astr. Soc.,* **229**, 31P.
Czyzak, S.J., Aller, L. H., Euwema, R. N. 1974, *Astrophys. J., Suppl. Ser.,* **28**, 465.
de Robertis, M. M., Dufour, R. J., Hunt, R. W. 1987, *J. R. astr. Soc. Canada,* **81**, 195.
Drake, S. A., Ulrich, R. K.1980, *Astrophys. J., Suppl. Ser.,* **42**, 351.
Dufay, J., Bloch, M., Bertaud, G., Dufay, M. 1964, *Ann. Astrophys.,* **27**, 555.
Evans, A., Callus, C. M., Albinson, J. S., Whitelock, P. A., Glass, I. S., Carter, B., Roberts, G. 1988, *Mon. Not. R. astr. Soc.,* **234**, 755.
Ferland, G. J.1979,*Astrophys. J.,***231**, 781.
Garcia, M. R. 1986, *Astr. J.,* **91**, 1400.
Gorbatskii, V. G. 1972, *Sov. Astr.,* **16,** 32.
Gorbatskü, V. G. 1973, *Sov. Astr.,* **17**, 11.
Griffin, R., Thackeray, A. D. 1958, *Observatory,* **78,** 245.
Hjellming, R. M., van Gorkom, J. H., Taylor, A. R., Seaquist, E.R., Padin, S., Davis, R. J., Bode, M. F.1986, *Astrophys. J.,* **305**, L71.
Hummer, D. G., Storey, P,J. 1987, *Mon. Not. R. astr. Soc,* **224**, 801.
Jacobs, V. L., Davis, J., Kepple, P. C, Blaha, M. 1977, *Astrophys. J.,* **211**, 605.
Joy, A. H., Swings, P. 1945, *Astrophys. J.,* **102**, 353.
Kastner, S. O. 1976, *Sol. Phys.,* **46,** 179.
Kastner, S. O. 1977, *Astr. Astrophys.,* **54**, 255.
Kastner, S. O., Bhatia, A, K. 1979, *Astr. Astrophys.,* **71**, 211.
Krautter, J., Williams, R. E.1988, *ESO Messenger,* No. 54, 33.
Krolik,J. H., McKee, C. F.1978, *Astrophys. J., Suppl. Ser.,* **37**, 459.
Landini, M., Fossi, B.C. M. 1972, *Astr. Astrophys., Suppl. Ser* .**,7,** 291.
Livio, M., Truran, J.W., Webbink, R. F. 1986, *Astrophys. J*., **308**,736.

Martin, P. G. 1988, in *Classical Novae,* Eds M. F. Bode & A. Evans, John Wiley (in press).
Mason, H. E. 1975, *Mon. Not. R. astr. Soc.,* **170**, 651.
Mason, K. O., Cordova, F. A., Bode, M. F., Barr, P. 1987, in *RS Ophiuchi* (1985) *and the Recurrent Nova Phenomenon,* Ed. M. F. Bode, VNU Science Press, Utrecht, p. 167.
Meinel, A. B., Aveni, A. F., Stockton, M. W. 1975, *Catalogue of Emission Lines in Astrophysical Objects,* Tech. Rep. No. 27, Optical Science Centre, Univ. Arizona, Tuscon.
O' Brien, T. J., Kahn, F. D. 1987, *Mon. Not. R. astr. Soc.,* **228**, 277.
Osterbrock, D. E. 1974, *Astrophysics of Gaseous Nebulae,* W. H. Freeman, San Francisco.
Prabhu, T. P., Anupama, G. C, Giridhar, S. 1987, *Bull. astr. Soc. India,* **15**, 98.
Rosino, L. 1987, in *RS Ophiuchi* (1985) *and the Recurrent Nova Phenomenon,* Ed. M. F. Bode, VNU Science Press, Utrecht, p. 1.
Rosino, L., Iijima, T. 1987, in *RS Ophiuchi* (1985) *and the Recurrent Nova Phenomenon,* Ed. M. F. Bode, VNU Science Press, Utrecht, p. 27.
Snijders, M. A. J. 1987, in *RS Ophiuchi* (1985) *and the Recurrent Nova Phenomenon,* Ed. M. F. Bode, VNU Science Press, Utrecht, p. 51.
Starrfield, S.., Sparks, W. M., Truran, J. W. 1985, *Astrophys. J.,* **291**, 136.
Taylor, A. R., Davis, R. J., Porcas, R. W., Bode, M. F. 1989, *Mon. Not. R. astr. Soc.,* **237**, 81.
Wallerstein, G., Garnavich, P. M. 1986, *Publ. astr. Soc. Pacific,* **98**, 875.

Note added in proof

In a recent paper, H. M. Schmid (1989, *Astr. Astrophys.,* 211, L31) suggests that 6830 Å feature arises due to Raman scattering of O VI 1032 line by neutral hydrogen in its ground state. O VI 1038 line, which forms a doublet with O VI 1032, Raman scattered by neutral hydrogen, gives rise to 7088 Å feature. This feature is blended with He I 7065, but can be identified in the spectrum of 1985 April 9 (Rosino & Iijima 1987, Fig. 5).